



# Simulations of the mid-Pliocene Warm Period using two versions of the NASA/GISS ModelE2-R Coupled Model

M. A. Chandler<sup>1,2</sup>, L. E. Sohl<sup>1,2</sup>, J. A. Jonas<sup>1,2</sup>, H. J. Dowsett<sup>3</sup>, and M. Kelley<sup>2,4</sup>

<sup>1</sup>Center for Climate Systems Research at Columbia University, New York, New York, USA

<sup>2</sup>NASA Goddard Institute for Space Studies, New York, New York, USA

<sup>3</sup>Eastern Geology & Paleoclimate Science Center, US Geological Survey, Reston, Virginia, USA

<sup>4</sup>Trinnovim LLC, 2880 Broadway, New York, New York 10025, USA

Correspondence to: M. A. Chandler (mac59@columbia.edu)

Received: 31 July 2012 – Published in Geosci. Model Dev. Discuss.: 13 September 2012

Revised: 14 March 2013 – Accepted: 21 March 2013 – Published: 24 April 2013

**Abstract.** The mid-Pliocene Warm Period (mPWP) bears many similarities to aspects of future global warming as projected by the Intergovernmental Panel on Climate Change (IPCC, 2007). Both marine and terrestrial data point to high-latitude temperature amplification, including large decreases in sea ice and land ice, as well as expansion of warmer climate biomes into higher latitudes. Here we present our most recent simulations of the mid-Pliocene climate using the CMIP5 version of the NASA/GISS Earth System Model (ModelE2-R). We describe the substantial impact associated with a recent correction made in the implementation of the Gent-McWilliams ocean mixing scheme (GM), which has a large effect on the simulation of ocean surface temperatures, particularly in the North Atlantic Ocean. The effect of this correction on the Pliocene climate results would not have been easily determined from examining its impact on the preindustrial runs alone, a useful demonstration of how the consequences of code improvements as seen in modern climate control runs do not necessarily portend the impacts in extreme climates.

Both the GM-corrected and GM-uncorrected simulations were contributed to the Pliocene Model Intercomparison Project (PlioMIP) Experiment 2. Many findings presented here corroborate results from other PlioMIP multi-model ensemble papers, but we also emphasise features in the ModelE2-R simulations that are unlike the ensemble means. The corrected version yields results that more closely resemble the ocean core data as well as the PRISM3D reconstructions of the mid-Pliocene, especially the dramatic warming in the North Atlantic and Greenland-Iceland-Norwegian Sea,

which in the new simulation appears to be far more realistic than previously found with older versions of the GISS model. Our belief is that continued development of key physical routines in the atmospheric model, along with higher resolution and recent corrections to mixing parameterisations in the ocean model, have led to an Earth System Model that will produce more accurate projections of future climate.

## 1 Introduction

Climate simulations with versions of the NASA/GISS general circulation models have been used to explore the Pliocene as a potential future climate analogue since NASA and the USGS partnered on a data-model comparison project in the early 1990s (Rind and Chandler, 1991; Chandler and Rind, 1992; Chandler et al., 1994; Poore and Chandler, 1994). However, as with numerous other climate modelling studies, the GISS model has often underestimated the high degree of polar amplification seen in Pliocene proxy data, particularly in the North Atlantic Ocean, without resorting to levels of CO<sub>2</sub> that are extreme and which are not supported by other studies (Hansen and Sato, 2012; Pagani et al., 2010; Seki et al., 2010). To further complicate the issue, higher CO<sub>2</sub> levels lead to low-latitude sea surface temperature increases that are not supported by an increasing number of ocean core analyses from tropical locations, a finding which largely validates prior assertions that the Pliocene tropical sea surface temperatures (SSTs) were little changed from the modern. Still, the ability to compare warm-climate

simulations with data-supported global reconstructions is an advantage that is not afforded by future climate change scenarios. Many groups, therefore, continue to pursue a better understanding of the middle Pliocene as it provides climate scientists with one of the few warm-climate scenarios in which global and high-latitude temperatures were as warm as IPCC's future climate projections, and has continental and ocean basin configurations that approximate modern geography.

The experiments examined in this study were performed in conjunction with the Pliocene Model Intercomparison Project (PlioMIP) Experiment 2 (Phase 1), the coupled ocean-atmosphere simulation. A description of the experiment design can be found in Haywood et al. (2010, 2011) and the description of the large-scale features of the multi-model ensemble is found in Haywood et al. (2013). Specific model characteristics that affect experiment design and which are unique to the NASA/GISS modelling effort are described below.

## 2 PlioMIP experiment design

For PlioMIP, a set of environmental reconstructions of the mid-Piacenzian Stage was compiled to form the PRISM3D reconstruction (Dowsett et al., 2010a). These reconstructions are distributed by the US Geological Survey as a series of uniformly gridded ( $2^\circ \times 2^\circ$ ) datasets, and constitute the preferred PlioMIP experiment protocol (Haywood et al., 2010, 2011). The adaptation of these datasets into boundary conditions for use with GISS ModelE2-R, as well as the creation of required related inputs, is described below.

### 2.1 Land/ice topography and ocean bathymetry

A reconstructed topography and land/sea mask for the Pliocene (Sohl et al., 2009), reflecting a 25-m rise in sea level compared to the modern, was developed as part of the PRISM3D effort. Elevation and areal distribution information for static representations of the Greenland Ice Sheet and East Antarctic Sheet (Hill et al., 2007) are incorporated into the topography, as the ice sheets must essentially be represented as “big white plateaus” for models that do not have dynamic land ice capabilities. The original  $2^\circ \times 2^\circ$  PRISM3D gridded topographic dataset was regridded in two ways for use with GISS ModelE2-R: once to  $2^\circ$  latitude  $\times$   $2.5^\circ$  longitude for the atmosphere component of the model, and further to  $1^\circ$  latitude  $\times$   $1.25^\circ$  longitude for the ocean component; for the land/sea mask, both atmosphere and ocean grids are non-fractional. The topographic relief from the resulting higher-resolution dataset is used directly as the input boundary condition, and is not applied as an anomaly relative to the modern as described in Haywood et al. (2010). Corrections to the resulting land-sea masks at both resolutions were made by hand to ensure that continental outlines were consistent

after regridding, that larger islands did not disappear as a result of the interpolation used in the regridding process, and that narrow ocean passages that existed in the Pliocene remained open. Note that in ModelE2-R, a straits parameterisation is used to maintain ocean flow through grid cell locations where straits cannot be resolved at the  $1^\circ \times 1.25^\circ$  resolution of the land/sea mask in the ocean component of the model. The changes to the land/sea mask introduced by the 25-m sea level rise removed the need to parameterise certain straits, since the straits could now be resolved; in these locations, Pliocene ocean waters flow freely. (See Table 1 for a comparison to the modern).

Note that the entire West Antarctic Ice Sheet is absent in our reconstruction (as per Pollard and DeConto, 2009), creating an “Ellsworth Passage” that separates the modern Antarctic Peninsula from the rest of Antarctica. The Pliocene ocean bathymetry in this region is uncertain, since we do not know what the thickness of any previous West Antarctic Ice Sheet may have been, nor whether the region was still undergoing glacio-isostatic adjustment after the loss of such ice. The current depth to bedrock in the region varies from 500 to 2000 m (Lythe et al., 2000); we used a uniform depth of approximately 500 m as a reasonable estimate for maximum ocean depth through the passage during the Pliocene.

Ocean bathymetry for the Pliocene was otherwise adapted from the modern, with most modifications made to accommodate continental edges flooded by the increase in sea level.

### 2.2 Riverflow and continental drainage

The river drainage system of the continents for the Pliocene experiments is similar to that of modern geography, but exceptions exist that cannot be prescribed based on the available paleogeographic evidence. For example, adjustments related to the coastal slope changes are required due to the sea level rise of 25 m, which was prescribed as consistent with reductions of ice sheet volume. Using the topographic elevation boundary condition array, and working inward from continental edges, we calculate the slope of each continental grid cell in eight directions (four sides, four corners). Runoff is then removed from each cell in the direction of maximum slope, tracing a route back to the coast. For coastal grid cells that have more than one border adjacent to an ocean grid cell, runoff crosses the coastal grid cell on the same trajectory as in the adjacent inland grid cell.

Glacial ice melts directly from the Greenland and East Antarctic ice sheets, and enters the surface ocean in prescribed cells wherever the edges of the ice sheets coincide with continental edges.

### 2.3 Ocean temperatures and salinity

Both the sea surface and deep ocean temperature datasets provided with PRISM3D (Dowsett et al., 2009, 2010b) were regridded to  $1^\circ$  latitude  $\times$   $1.25^\circ$  longitude horizontal

**Table 1.** Use of straits parameterisations in GISS ModelE2-R – Modern vs. Pliocene.

Strait Name	Geographic Location	Depth (m)	Width (m)	Modern	Pliocene
Dolphin & Union	Between Victoria Island and mainland Canada, Northwest Territories/Nunavut	56	32 000	parameterised	explicit
Dease	Between Victoria Island and the Kent Peninsula, Nunavut, Canada	56	25 000	parameterised	explicit
Fury & Hecla	Between Baffin Island and the Melville Peninsula, Nunavut, Canada	30	15 000	parameterised	parameterised
Nares	Between Ellesmere Island, Canada and Greenland	202	30 000	parameterised	parameterised*
Gibraltar	Between Spain and Morocco	280	15 000	parameterised	explicit
English	Between England and France	30	35 000	parameterised	explicit
Dardanelles	Northwestern Turkey	30	1000	parameterised	parameterised
Bosporous	Northwestern Turkey	30	2000	parameterised	explicit
Bab al-Mandab	Connects Red Sea and Gulf of Aden	140	25 000	parameterised	parameterised
Malacca	Between Malay Peninsula and Sumatra, Indonesia	30	40 000	parameterised	parameterised
Selat Sunda	Between Java and Sumatra, Indonesia	30	25 000	parameterised	parameterised

\* The Nares Strait is divided into two parts to accommodate Pliocene geography.

resolution; the vertical resolution of the deep ocean temperature dataset was maintained at 33 layers. Wherever there were missing values within the regridded temperature dataset with respect to our new ocean bathymetry, we used a “nearest neighbour” approach to fill the gaps, always maintaining the integrity of the vertical temperature profile. Salinity values for the Pliocene were derived from modern salinity values (Conkright et al., 1998), with missing values filled in in the same fashion as the temperatures.

#### 2.4 Biome distribution mapping to GISS ModelE2-R vegetation categories

GISS ModelE2-R uses a vegetation scheme that includes eight vegetation types, plus land ice as an additional type. Each type is used in to define or modify certain physical characteristics of the land surface and ground, such as visible and near-infrared surface albedo, the water holding capacity of soil layers, transpiration rates and snow masking depths. The GISS vegetation categories were originally distilled from a more detailed global vegetation compilation of Matthews (1983, 1984), and subsequently have been modified to better reflect agricultural coverage and its impact. Irrigation effects are not included. The GISS model’s radiation code also accounts separately for subgrid-scale fractions of bare ground in each cell.

The prescribed Pliocene biome distributions for PlioMIP were developed by the British Antarctic Survey (BAS biomes and mega-biomes; Salzmann et al., 2008), with each participating modelling group being responsible for developing a method of translation appropriate for their model’s vegetation parameterisation. To make this translation for the GISS model, we regridded the BAS modern mega-biome distribution to  $2^\circ$  latitude  $\times$   $2.5^\circ$  longitude (the standard resolution

**Table 2.** Correlation of BAS mega-biomes with GISS ModelE2-R modern vegetation classes.

BAS Mega-Biome Type	GISS Vegetation Type
Tropical Forest	Rainforest
Warm-Temperate Forest	Deciduous forest
Savanna/dry woodland	Grassland
Grassland/dry shrub	Grassland
Desert	Desert
Temperate forest	Deciduous forest
Boreal forest	Evergreen forest
Tundra	Tundra
Dry tundra	Tundra

for the ModelE2-R vegetation input), and then compared the BAS distribution cell by cell against the GISS modern vegetation distribution used for ModelE2-R. We then used a frequency distribution chart plotting BAS vs. GISS types to identify dominant links between types (see Table 2), and the BAS Pliocene mega-biome distribution was translated accordingly, with non-fractional values assigned to each cell. Note that under this translation scheme, the GISS vegetation types shrub/grassland and tree/grassland have no clear corollary to the BAS mega-biomes, and instead are represented by grassland alone.

#### 2.5 NASA/GISS ModelE2-R

The climate model used for these simulations was developed at the NASA Goddard Institute for Space Studies (GISS) and is the CMIP5/PMIP3 version that will be archived as GISS ModelE2-R for IPCC AR5 and PMIP. The suffix (-R) is used by GISS to identify the specific ocean version in the coupled

model, in this case the Russell ocean model. The physics and parameterisations of the model are described in Schmidt et al. (2006) and updates for AR5 are being described in Schmidt et al. (2012, 2013). The most recent documentation is also available through the NASA/GISS website. This model is part of a multi-decade code lineage developed at NASA/GISS and which has been referred to in the literature over the years as Model II', si1995, si1997 and si2000 (e.g., Hansen et al., 2000, 2002) and afterward as ModelE. Henceforth, in this paper we will refer to the model as ModelE2-R, or ModelE2 if we are describing the atmosphere-only version.

ModelE2-R calculates temperature, pressure, winds and specific humidity as prognostic variables, using the conservation equations for mass, energy, momentum and moisture. The standard configuration produces global climate simulations at a latitude  $\times$  longitude resolution of  $2.0^\circ \times 2.5^\circ$  in the atmosphere,  $1.0^\circ \times 1.25^\circ$  in the ocean, and includes 40 layers in the atmosphere and 32 layers in the fully coupled dynamic ocean (Russell et al., 1995). ModelE2 (atmosphere only) uses second-order differencing schemes in the momentum and mass equations and a quadratic-upstream scheme for heat and moisture advection, which implicitly enhances an absolute model resolution of  $2.0^\circ \times 2.5^\circ$  grid to  $0.7^\circ \times 0.8^\circ$  (Schmidt et al., 2006, Table 1). The radiation physics includes calculations for trace gas constituents ( $\text{CO}_2$ ,  $\text{CH}_4$ ,  $\text{N}_2\text{O}$ , CFCs,  $\text{O}_3$ ) and aerosols (natural and anthropogenic) and is capable of simulating the effects of large forcing changes in constituents such as volcanic aerosols and greenhouse gases. The forcings are assigned at startup or can be altered transiently throughout an experiment. In addition, a parameterised gravity wave drag formulation incorporates gravity-wave momentum fluxes that result from flow over topography and deformation in baroclinic systems. The generation, propagation and drag are all a function of the calculated variables at each grid box for the various vertical levels. New to this model is the capability of running with interactive atmospheric chemistry, aerosols and dust concentrations, as well as the incorporation of a model-calculated (rather than parameterised) first aerosol indirect effect. ModelE2-R also employs a prognostic cloud water parameterisation (Del Genio et al., 1996; Schmidt et al., 2006, 2012) that represents all-important microphysical processes.

## 2.6 Corrections to the ocean mixing scheme

It is important to emphasise that the simulations described here as “GM-CORR” utilise a correction to the Gent-McWilliams parameterisation in the ocean component of the coupled climate model. In prior implementations of the mesoscale mixing parameterisation in GISS ModelE, which like many ocean models uses a unified Redi/GM scheme (Redi, 1982; Gent and McWilliams, 1990; Gent et al., 1995; Visbeck et al., 1997), a miscalculation in the isopycnal slopes led to spurious heat fluxes across the neutral surfaces,

resulting in an ocean interior generally too warm, but with southern high latitudes that were too cold. A correction to resolve the problem was made for this study, and it will also be employed in all subsequent versions of ModelE2-R going forward. In applying the correction the new code also uses a minimum eddy diffusivity of  $600 \text{ m}^2 \text{ s}^{-1}$  in the mesoscale eddy formulation. Since some multi-model ensembles have included the previous version we also present here a comparison of some of the more dramatic differences between the old and new simulations. In this paper, we refer to the uncorrected version of the model as “GM-UNCOR”. No other differences exist between the two simulations beyond the corrections to the mixing scheme. All boundary conditions, initial conditions and model physics are identical and there were no changes made to the land-sea masks or subgrid-scale strait definitions.

## 3 Simulation results

All results presented in the following sections are climatological averages for years 921–950 of our Pliocene and Preindustrial simulations. The sea surface temperatures used in the Preindustrial control run are from 1876–1885. As noted above in Sect. 2.6, the main results from the GISS ModelE2-R now include a correction to the ocean mixing scheme. Pliocene and Preindustrial runs including the correction are labeled “GM-CORR”; results that are from the uncorrected version of the model are labeled “GM-UNCOR”.

### 3.1 Sea surface and surface air temperature response

The most fundamental mismatch between warm climate paleoclimate simulations and paleoclimate proxy data has been the inability of simulations to achieve both a reduced pole-to-equator temperature gradient along with acceptable magnitudes of polar and tropical temperature amplification. Excessive greenhouse gas (GHG) levels have traditionally been required for climate models to achieve polar temperature amplification that is in the vicinity of the observed levels for the warmer time periods in Earth history. However, that same GHG excess tends to cause tropical temperatures that are unrealistically high.

Pliocene simulations are no different in this respect, including those for PlioMIP Experiment 2 (Haywood et al., 2013). However, PlioMIP Pliocene experiments prescribe the use of 405 ppmv  $\text{CO}_2$ , with other greenhouse gases held at preindustrial levels. Though 405 ppmv is actually on the upper end of proxy-based estimates for the Pliocene (Kürschner et al., 1996; Raymo et al., 1996; Pagani et al., 2010), that level is relatively low from the perspective of other warm Tertiary and Mesozoic climates. The problem of tropical temperature amplification in Pliocene simulations is thus less of a conundrum than for most past warm periods. Given that there are still large uncertainties associated with pre-

ice core CO<sub>2</sub> estimates, and given that the tropical energy balance is very sensitive to even small CO<sub>2</sub> changes, the simulated tropical SSTs are within the envelope of uncertainties. All the same, the warming in mid- to high latitudes is supplemented substantially by the direct forcing and feedbacks associated with the additional carbon dioxide; 405 ppmv is, after all, 45 % higher than the 280 ppmv value used in most preindustrial control runs. Of course, high-latitude temperatures are impacted by the specified sea ice and ice sheet distributions, which are substantially decreased compared with the present day (Hill et al., 2007; Dowsett et al., 2010b); however, compared to the CMIP3 model results and previous GISS model simulations of the Pliocene (e.g., Chandler et al., 1994; Shukla et al., 2009, 2011; Haywood et al., 2013), the GM\_CORR version of the GISS ModelE2-R shows compelling improvement. In the final analysis, the corrected simulation results for PlioMIP Experiment 2 yield sea surface temperatures in the North Atlantic that are closer to PRISM3D core data than those that we previously contributed to the multi-model ensemble of Dowsett et al. (2012) (see cool bias in the North Atlantic region of Fig. 3e from Dowsett et al., 2012).

### 3.2 Global and zonal average temperatures

The global warming compared to preindustrial simulations is similar in both Pliocene simulations (Table 3) at 2.25 °C for the Pliocene GM\_CORR and 2.12 °C for Pliocene GM\_UNCOR. Zonal average sea surface and surface air temperature anomalies (SST and SAT in Fig. 1) for the Pliocene GM\_CORR simulation peak over the regions of sea ice loss and ice sheet reduction. The surface air temperatures are slightly warmer than the multi-model ensemble averages for all PlioMIP models in both the Northern (+8.2 °C) and Southern (+9.1 °C) Hemispheres (see Haywood et al., 2013). At low latitudes the character of the SAT temperature anomalies are similar between the GM\_CORR and GM\_UNCOR versions of the model. However, the ocean mixing correction has decreased zonal average temperatures in the extratropics of the Southern Hemisphere while increasing temperatures in the Northern Hemisphere. The significant exception is in the northern high latitudes, where surface air temperatures in GM\_CORR are warmer than in GM\_UNCOR by at least 2 °C at all latitudes north of 50° N.

High latitude amplification of the sea surface temperature anomaly is asymmetrical, with more than twice as much warming in the Northern Hemisphere (+4.5 °C) as in the Southern Hemisphere (+2.2 °C) in GM\_CORR. The peak of the zonal average SST falls at 65° N, at the high end of the range of PlioMIP models, and slightly exceeds the PRISM3D data for that latitude. Sea surface temperatures in GM\_CORR are up to 9 °C warmer in the North Atlantic than in the uncorrected model at their peak (Fig. 2); in fact, zonal average SSTs in the corrected model are warmer than at any other location. In contrast, at similar latitudes the peak SST

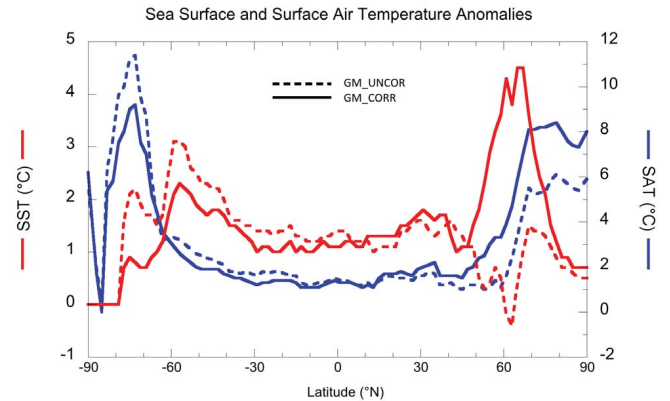


**Fig. 1.** Zonal average anomalies of surface air temperature (in blue) and sea surface temperature (in red). The simulated high-latitude amplification of surface air temperature and the peak SSTs around 65° N are more similar to proxy data than those produced by the earlier GM\_UNCOR version of the GISS ModelE2-R, but tropical temperature anomalies in both versions are still slightly higher than data interpretations for the mid-Pliocene.

anomalies in the uncorrected model actually showed cooling compared to their preindustrial counterpart. The regional aspects of this large difference caused by the ocean mixing correction will be discussed below.

The correction to the ocean mixing scheme clearly is a substantial improvement on the previous GM\_UNCOR Pliocene simulation, which was too cool, zonally averaged, at high northern latitudes due to the large cooling in the North Atlantic. The peak SST warming in the Southern Ocean and the 1–2 °C zonal average increase across southern mid-latitudes are broadly similar to proxy data in the region, which show little longitudinal variation and yield temperature increases in the same range.

Tropical zonal average SAT anomalies are approximately 1.1 °C and sea surface temperatures in the tropics are similarly amplified, with a zonal average warming of 1.2 °C just north of the equator. Both corrected and uncorrected models yield broadly similar results in the tropics. The values fall on the low side of the range of PlioMIP model results for the region, but remain a bit warmer than the PRISM3D reconstruction, which is barely elevated above late 20th century tropical temperatures within 10° of the equator.

### 3.3 Regional temperature changes: North Atlantic and Arctic oceans

Using a four-model subset of the PlioMIP group of climate models (including the Pliocene GM\_UNCOR version of ModelE2-R), Dowsett et al. (2012) generated a mean SST field to compare with the PRISM3 ocean core proxy data. They reported several regional differences between proxy data and simulation results, but the most pronounced mismatch of models and data was in the underestimate of North

**Table 3.** Global mean climate variables for Pliocene and Preindustrial simulations

	GM_CORR	GM_UNCOR	Difference	GM_CORR	GM_UNCOR	Difference
Surface Air Temperature (°C)				H <sub>2</sub> O of Atmosphere (mm)		
Pliocene	16.21	16.29	−0.08	25.99	25.91	0.08
Preindustrial	13.96	14.17	−0.21	22.74	22.66	0.08
Difference	2.25	2.12	0.13	3.25	3.25	0.00
Planetary Albedo (%)				Precipitation (mm day <sup>−1</sup> )		
Pliocene	28.87	28.72	0.15	3.34	3.34	0.00
Preindustrial	29.71	28.55	1.16	3.17	3.17	0.00
Difference	0.84	0.17	−1.01	0.17	0.17	0.00
Snow Coverage (%)				Evaporation (mm day <sup>−1</sup> )		
Pliocene	7.67	7.3	0.37	3.34	3.34	0.00
Preindustrial	9.96	9.26	0.70	3.17	3.17	0.00
Difference	−2.29	−1.96	−0.33	0.17	0.17	0.00
Snow Depth (mm H <sub>2</sub> O)				Total Cloud Cover (%)		
Pliocene	12.8	12.12	0.68	59.51	59.28	0.23
Preindustrial	10.35	9.72	0.63	61.76	61.51	0.25
Difference	2.45	2.40	0.05	−2.25	−2.23	−0.02
Global Ocean Ice Cover (%)				Moist Convective Cloud Cover (%)		
Pliocene	3.14	2.72	0.42	4.2	4.25	−0.05
Preindustrial	4.71	3.96	0.75	4.08	4.15	−0.07
Difference	−1.57	−1.24	−0.33	0.12	0.10	0.02
Arctic Ice Cover (%)				Southern Ocean Ice Cover (%)		
Pliocene	3.40	4.04	−0.64	2.87	1.41	1.46
Preindustrial	5.71	5.29	0.42	3.72	2.62	1.1
Difference	−2.31	−1.25	−1.06	−0.85	−1.21	0.36

Atlantic temperature change by the models (see Fig. 3e, Dowsett et al., 2012). The North Atlantic SST anomalies produced by the GISS model before applying the ocean mixing correction (GM\_UNCOR) were by far the least representative of the proxy data, actually exhibiting cooling, whereas most models produce some warming in the North Atlantic (though not enough to match data). The results using ModelE2-R with the corrected ocean mesoscale mixing scheme (GM\_CORR) are much warmer in the North Atlantic (Fig. 2), actually exhibiting more warming in that region than any other model in the PlioMIP multi-model ensemble. Yet, GM\_CORR still exhibits small regional cooling in the upper mid-latitude Atlantic, a bias also seen in the preindustrial simulations as compared to observed SST climatologies of the late 19th century (see Dowsett et al., 2012 Fig. 3d).

Despite minor differences in the zonal average anomalies compared to previous GISS model simulations, the zonal values are soundly within the range defined by the PlioMIP model ensemble for zonal temperature results. However, examination of the regional temperature fields shows significant basin-to-basin differences and the substantial improvements that the ocean mixing scheme correction has yielded.

In the previous GM\_UNCOR version of the model (Fig. 3a) the dominant feature in the SST anomaly field was the strong cooling in the North Atlantic Ocean. The cooling peaked in the central North Atlantic around 60° N, but was broadly distributed throughout the North Atlantic, from the coast of Nova Scotia, to the Norwegian Sea, extending along the return gyre all the way to Africa and into the tropical flow. The Arctic experienced a broad 1–2 °C warming, less than most other regions of the ocean.

In stark contrast, the ocean mixing scheme correction leads to an intense SST warming in the Pliocene GM\_CORR version of the model (Fig. 3b). The warm anomaly peaks in the Norwegian and Iceland sectors of the GIN Sea at +9.7 °C and extends uninterrupted to the south of Greenland into the Labrador Sea, where another peak exceeds +6 °C in the Atlantic Ocean east of Newfoundland. These very high anomalies do not, however, extend far into the Arctic Ocean, where the 1–2 °C warming is similar to that seen in the GM\_UNCOR version of the model. The warm anomaly in the GIN Sea spreads southward, following the return flow of the North Atlantic gyre as it merges with the Canary Current, though the values are only about half as large in this region

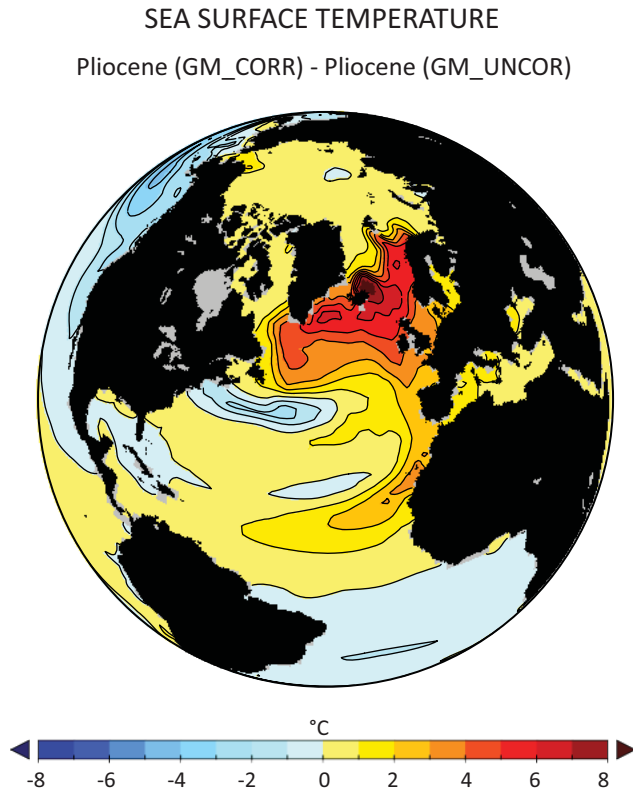


**Fig. 2.** Corrections to the ocean mesoscale mixing scheme (GM\_CORR) yield substantially warmer sea surface temperatures in the North Atlantic, closer to what ocean core data suggest. Although even GM\_CORR still exhibits small regional cooling in the upper mid-latitude Atlantic, a bias also seen in the multi-model ensemble, preindustrial simulations as compared to observed preindustrial SST climatologies (1870–1900; see Dowsett et al., 2012 Fig. 3d).

as in the PRISM3D data (3–4 °C as opposed to 6–8 °C), whereas further north the peak values more closely resemble the ocean core data. In comparing the simulated warming to the core data poleward of 75° N, the model warming is also 2–4 °C too cool, but again the new simulation compares far more favourably to data reconstructions than the Pliocene simulation that was run with the uncorrected CMIP5 version of the model and is even an improvement compared to coarser resolution CMIP3 GISS ModelE-R simulations (not shown). Noticeably, the most pronounced negative temperature anomaly in the Pliocene ocean also lies in the North Atlantic in GM\_CORR, though the geographic character is unlike the cool anomaly in the GM\_UNCOR results (compare Fig. 3a and b). Figure 3b shows a region of cooling that is narrow in latitudinal extent, but spanning nearly the width of the Atlantic Ocean, tracing the regional expression and extent of the modern Gulf Stream Current.

Delayed warming is characteristic of the North Atlantic region in many warm-climate coupled model simulations,

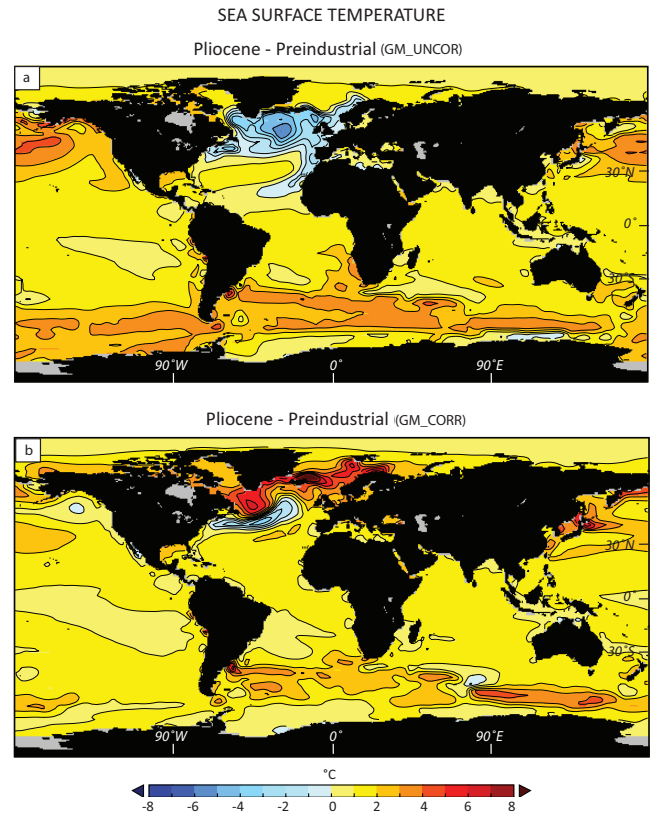


**Fig. 3.** The sea surface temperature anomaly field from the Pliocene simulations compared to their respective preindustrial control runs. The anomalies show a generally warmer planet with high-latitude amplification of SSTs. The most apparent feature is the large temperature change in the North Atlantic and, especially, the dramatic warming that results when the corrected ocean mixing scheme is applied. The North Atlantic and Southern Ocean warm anomalies are key fingerprints of the mid-Pliocene Warm Period as reconstructed by the US Geological Survey PRISM3D Project, suggesting that the corrected version of ModelE2-R (GM\_CORR in the text) is a great improvement over the uncorrected version (GM\_UNCOR) and is also an advance compared to simulations that used the coarser-grid CMIP3 version of GISS ModelE.

including the PlioMIP ensemble simulations (compare Figs. 2a and 3a from Haywood et al., 2013) and the future climate change simulations documented in the IPCC's Fourth Assessment Report (AR4; IPCC, 2007, see Fig. 10.8). In addition, the North Atlantic is one of the few regions where inter-model standard deviation exceeds the mean of the multi-model ensembles (Haywood et al., 2013; Meehl et al., 2007, see Figs. 10.8 and 10.9) revealing just how much our best models differ, and how great the uncertainty is regarding climate change in this critical region. It is not surprising then that simulations of the mid-Pliocene conducted using coupled ocean-atmosphere models have rarely achieved adequate simulations of the North Atlantic Ocean. Ocean core data and, therefore, PRISM3D reconstructions, have shown with considerable confidence that the North

Atlantic and northward extensions into the GIN Sea experienced strong warming in the Pliocene – greater than anywhere else in the global oceans and greater than in other experiments in the multi-model PlioMIP ensemble (Haywood et al., 2013; see Fig. 3). Dowsett et al. (2012) point out that even accounting for a cool bias in the models compared to their own preindustrial control simulations, coupled models underestimate North Atlantic warming in the mid-Pliocene by 2–8 °C.

### 3.4 Regional ocean temperature changes: North Pacific, Southern Ocean, and the Tropics

Temperature change throughout the rest of the global oceans is muted by comparison with the North Atlantic and Arctic, but there are still significant anomalies that can be compared and contrasted to data reconstructions in other key oceanic regions. The North Pacific and Southern Ocean show warming in the Pliocene in both the GM\_CORR and GM\_UNCOR simulations (Fig. 3a and b). Unlike the Atlantic anomalies, the sea surface temperatures in the Pacific and Southern Oceans are broad and peak below +5 °C. In addition, the warming was 2–4 °C less once the ocean mixing scheme was corrected. More extreme warm anomalies near the Asian shoreline in the northwest Pacific are supported by ocean core data that Dowsett et al. (2012) give a confidence rating of “Very High”. It is noteworthy that the temperature anomaly lessens poleward of 45° N latitude and into the northeastern Pacific Ocean in the GM\_CORR model. Data from the Gulf of Alaska do not dispute that trend. Cores taken off the west coast of North America are given a “high-confidence” rating in PRISM project analyses and indicate levels of Pliocene warming that are not simulated by the corrected version of the model.

While mid- to high latitude warming is evident in ocean cores throughout the Southern Ocean there is little longitudinal variation in the warming – despite the absence of the West Antarctic Ice Sheet in the Pliocene boundary conditions. ModelE2-R, like the multi-model PlioMIP ensemble, shows that the South Atlantic and southern Indian Ocean regions are somewhat warmer than the corresponding latitudes in the South Pacific. This feature tends to be robust, and is also borne out by the PRISM3D reconstructions. The results with GM\_CORR appear to be an improvement compared to GM\_UNCOR, which had broad warming throughout the southern high latitudes. However, ocean core data is very limited at many longitudes in the Southern Ocean and the meridional character of the Pliocene Southern Hemisphere sea surface temperatures is not well understood.

Tropical temperature change, as mentioned previously, has proven to be a dilemma for many model-data comparisons for past warm periods in Earth history. One of the overarching themes from proxy studies of pre-Pleistocene warm climates is that tropical temperatures have been relatively stable compared to higher latitudes, resulting in decreased

meridional temperature gradients (e.g., Zachos et al., 1994; Galfetti et al., 2007; Pearson et al., 2007; Dowsett et al., 1996, 2010b). In contrast, climate model simulations of these past time periods show that when the forcing is either a well-mixed greenhouse gas or the result of changes to solar insolation, tropical temperatures respond measurably (e.g., Rind and Chandler, 1991; Chandler et al., 1994; Sloan et al., 1996; Haywood et al., 2000; Jiang et al., 2005).

The mid-Pliocene, with its relatively lower levels of atmospheric CO<sub>2</sub> (compared to earlier warm periods in geologic history), has minimal additional forcing in the tropics, thus, tropical SSTs and surface air temperatures warm only about 1 °C relative to the preindustrial. Tropical temperatures warmed another a degree in the Atlantic Ocean when the ocean mixing was corrected, but that was related to the fact that the uncorrected model received substantial cool surface flow from the unrealistic cold anomaly in the North Atlantic. Otherwise there was little change in response in the tropics between GM\_CORR and GM\_UNCOR.

Results from the PRISM analyses show that some tropical regions may in fact have experienced warming on the order of 1–2 °C, but PRISM also includes a number of sites where no temperature increases are discernable. In each ocean basin, the sites that show little or no temperature change are in the central or western warm pools, whereas those sites with minor warming are generally in the easternmost portions of the basins. All of the ModelE2-R simulation results show generally uniform east-west temperature increases across all ocean basins and, where minor variations exist, there is no consistent east-west trend. This permanent El Niño or “El Padre” character of the tropical SSTs is consistent with some Pliocene data and simulations (Shukla et al., 2009 and references therein), but the issue is far from resolved with both data and modelling studies suggesting ENSO variability was still present in the Pliocene (Scropton et al., 2011; Watanabe et al., 2011).

### 3.5 Arctic sea ice

The impact of the Pliocene warming on Arctic sea ice is of special interest because of the continuing degradation of the present-day polar cryosphere related to greenhouse warming. Coupled model experiments calculate rather than specify the sea ice distribution, and although the initial conditions for these simulations include reduced ice, it is not clear that models can maintain such distributions with the 405 ppmv CO<sub>2</sub> levels used in the PlioMIP experiments. In the case of the GISS ModelE2-R experiments, however, the reduction is at least partially sustained: sea ice is reduced in both the GM\_CORR and GM\_UNCOR versions (Fig. 4 and Table 3). The corrected ocean mixing scheme shows sea ice is reduced by 40 % in the Arctic, which is nearly twice as before the correction was applied. (Note that in the Southern Hemisphere (maps not shown), the Pliocene ocean ice is also less compared to the preindustrial, but the ocean mixing



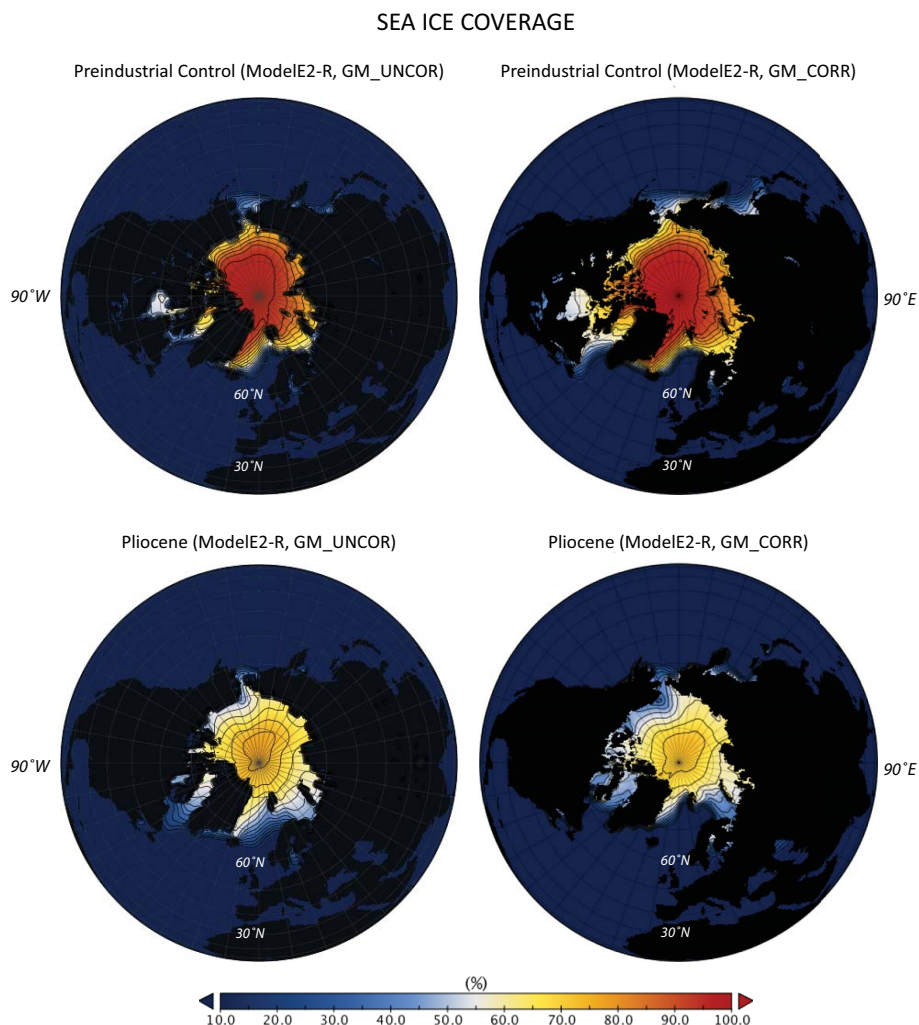


**Fig. 4.** Extent of sea ice cover from the two preindustrial simulations (top) and the mid-Pliocene simulations (bottom) for both the GM\_UNCOR and GM\_CORR versions of the model. Sea ice in the corrected Pliocene run is reduced by 40% in the Arctic Ocean and retreats on all margins, not just in the North Atlantic where SSTs warm the most. The reduction of ice was less before the ocean mixing scheme correction was applied, but the geographic character of ice reduction is similar. The central Arctic ice cap in the Pliocene no longer maintains a large geographic area where ice cover is above 90%. Ice thickness is greatly reduced as well, indicative of a loss of multi-year ice and suggesting that the region would be highly vulnerable to even moderate further increases in temperature.

correction actually reduces the amount of ice lost). Regardless, the geographic character of the reduction is very similar between both corrected and uncorrected versions of the model in the Arctic. Reductions of sea ice are greatest in the proximity of the GIN Sea warming, but decreased sea ice extent and thickness are pronounced everywhere around the Arctic ice cap, especially at the margins of the ice cap.

A further examination of the vertical temperature profile in the Atlantic and Arctic sector (Fig. 5) also shows that the remaining Arctic sea ice may be extremely vulnerable to even small amounts of additional warming. The Arctic Ocean warms considerably at depth and the sea ice cap thins dramatically as its areal coverage is reduced. No doubt these results are highly sensitive to the ocean-ice parameterisation in the

climate model. We explore that issue, along with the seasonal cycle of polar sea ice, in greater detail in a forthcoming paper where we will discuss further the impact of the corrected ocean mixing scheme on the deep ocean.

### 3.6 Atlantic meridional overturning circulation

One of the most significant differences of the Pliocene GM\_CORR simulations, compared with those of the uncorrected model, is the characteristic of the meridional overturning in the Atlantic Ocean. In GM\_UNCOR the Atlantic Meridional Overturning Circulation (AMOC) collapsed and did not recover, something that was expected to be related to problems with the ocean mixing scheme. Although we hesitate to state that this is a clear improvement (little direct

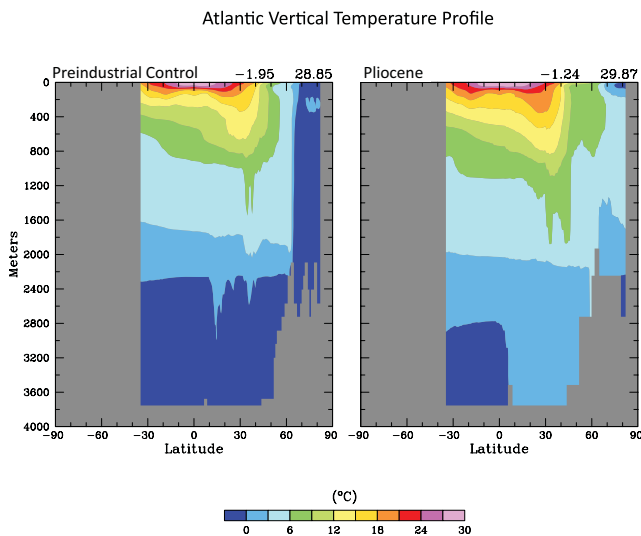


**Fig. 5.** The vertical profile of zonal average ocean temperatures in the Atlantic Ocean basin for the corrected (GM.CORR) Preindustrial control run (left) and the Pliocene simulation (right). Deep and bottom water temperatures warm, associated with reductions in Antarctic Bottom Water production (not shown) and increased production of North Atlantic Deep Water (see Fig. 6 and text). Warming at depth in the Arctic Ocean is also evident, leaving sea ice at the surface even more vulnerable to melting than the substantial 40 % ice cover reduction might suggest.

evidence from observations), it seems likely that the collapsed AMOC in the previous simulation was erroneous. It is also uncertain how the 25 % increase in the AMOC contributes to the warmer SSTs since the associated increase in ocean heat transports is only 4 % (Zhang et al., 2013).

The Atlantic mass stream function for GM.CORR is shown in Fig. 6 for both the preindustrial control and the Pliocene simulation. The peak overturning increases from 14.35 to 17.89 Sverdrups, a 25 % strengthening of the circulation, and the geographic location of the peak shifts poleward by 5–10° latitude. Also apparent is the formation of an overturning cell at about 70° N, which appears to derive deep water production from either the anomalously warm Iceland or Norwegian Seas (or both). Taken together with the vertical temperature profile shown in Fig. 5, this newly developed overturning cell may be the origin of warming ocean waters at depth in the Arctic Ocean. Further sensitivity experiments will be required to examine to what extent these features are driven by (1) the increased CO<sub>2</sub>, (2) the reduction of the Greenland Ice Sheet, (3) changes in freshwater flux associated with altered river outflow, and (4) what affect the 25-m sea level rise may have had on flow along coastlines or through subgrid-scale straits.

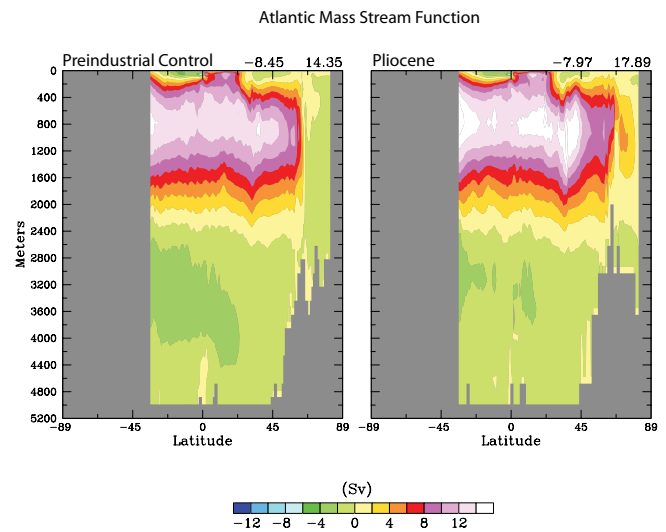


**Fig. 6.** Zonally averaged mass stream function in the Atlantic Ocean basin for the corrected (GM.CORR) Preindustrial (left) and Pliocene simulations (right). Peak overturning in the North Atlantic of the Pliocene strengthens by over 25 % compared to the preindustrial run, including an intrusion of a plume of water, with origins in the North Atlantic, to depths of over 1000 m in the Arctic Ocean. This increased overturning in the Pliocene has been hypothesised for years based on surface and deep water temperature proxies and estimates of NADW penetration relative to water masses from other basins. However, coupled climate models have rarely found this feature in Pliocene experiments.

#### 4 Hydrology

In most warm climate scenarios, the hydrological cycle strengthens as more water is evaporated from the oceans and the water holding capacity of the atmosphere increases. Surface heating destabilises air masses, increasing convective events leading to increases in precipitation rate, punctuated by longer periods of drying over land. Table 3 shows some of these effects on global hydrological variables as atmospheric water vapour, precipitation, evaporation and moist convection all increase in the Pliocene. Total cloud cover actually decreases slightly, a characteristic of some warm climate simulations (Wang and Lau, 2006; Haywood et al., 2009; Bender, 2011) and supported by recent observations (Liu et al., 2009; Tang et al., 2012). The ocean mixing scheme correction has, somewhat surprisingly, little effect on the hydrological cycle globally averaged. As mentioned, the Pliocene precipitation and evaporation rates increase globally in both GM.UNCOR and GM.CORR relative to the preindustrial. However, precipitation over continents in GM.CORR actually increases more than evaporation (see Fig. 7), leading to a net moisture gain of approximately 15 % over land. At the same time, precipitation and evaporation anomalies over land are highly variable and local effects dominate the moisture balance. The vast majority of continental regions show that

increased rainfall is offset by increased evaporation (compare Fig. 7b to c); similarly, decreasing precipitation over land is commonly accompanied by lower evaporation rates in the same region. Despite the distinct differences when the Pliocene is compared with the preindustrial, the similarity between both the uncorrected and corrected versions of ModelE2-R are striking. The only major differences that are apparent in the precipitation anomalies occur over the North Atlantic, where the uncorrected ocean mixing error leads to cooling temperatures (even compared to the preindustrial) and a dampened hydrological cycle. The precipitation and evaporation fields for GM\_CORR are fully consistent with the SST anomalies shown in Fig. 3.

Over ocean regions, however, this is not necessarily true. In particular, the subtropical oceans experience intensified drying, as regions of increased evaporation are commonly affected by declining precipitation (shown for GM\_CORR only). This effect is seen in the subtropics of the Pacific, Atlantic and Indian Oceans, as well as in both hemispheres. The implications for salinity distributions and the meridional overturning circulation may be significant. We are in the process of examining the impacts, and will discuss the findings in a future paper as further sensitivity experiments are completed.

## 5 Discussion of global feedbacks

The primary drivers behind the climate changes simulated in the ModelE2-R Pliocene simulations are threefold: (1) altered boundary conditions, including minor modifications to continental geography, orography and coastlines, (2) reduced Greenland and West Antarctic ice sheets, and the poleward extension of the Southern Ocean over West Antarctica; and (3) an increased atmospheric carbon dioxide level (405 ppmv). However, as with all warm climate experiments, the amplifying effects of feedbacks are fundamental to the evolution of the simulation and to the ultimate equilibrium state of the climate.

With global average temperatures increasing in the mid-Pliocene simulations more than  $2^{\circ}\text{C}$  compared to the preindustrial control runs and with the Northern Hemisphere warming more than the Southern Hemisphere ( $2.4^{\circ}\text{C}$  vs.  $2.1^{\circ}\text{C}$  in GM\_CORR) we look to changes in albedo and water vapour to explain much of the difference. All provide important positive feedbacks in the warmer Pliocene climates. The reduced planetary albedo in the Pliocene simulations is consistent across both Northern and Southern Hemispheres and is partly related to cloud cover reductions of a couple percent. Of course the ground albedo change is even more substantial ( $-20\%$  NH,  $-13\%$  SH), as snow and ice cover decrease dramatically in the warmer climate. The specified reduction of ice sheets imposes a decrease in ground albedo, although it is not as large an effect as the albedo change caused by the loss of the snow and ice cover, which

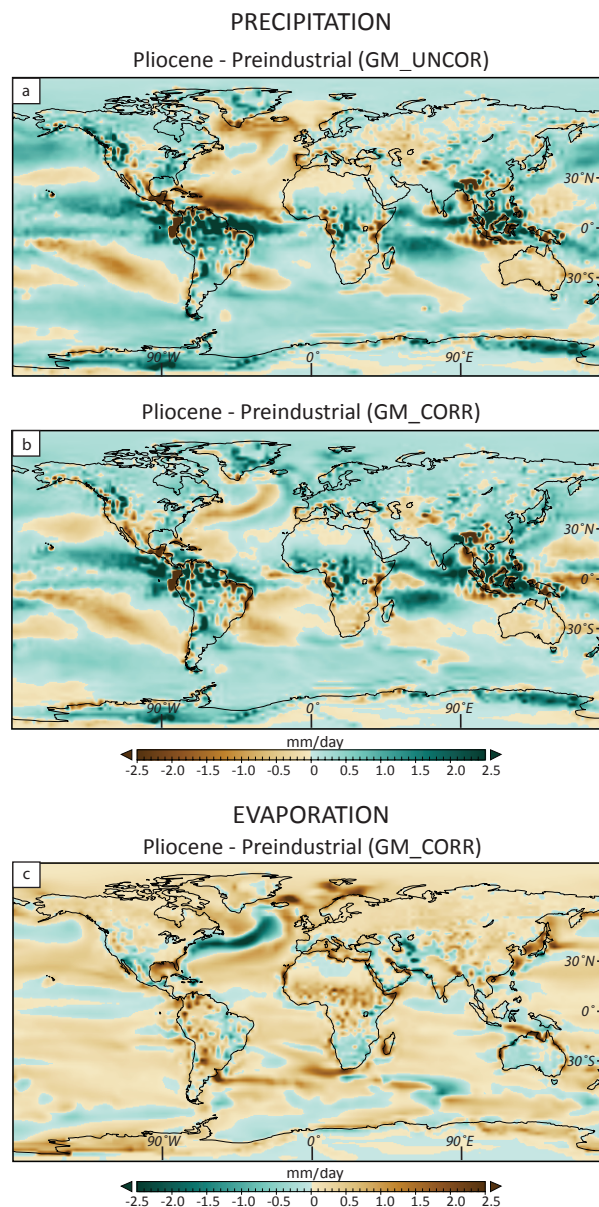


**Fig. 7.** Precipitation anomalies for both mid-Pliocene simulations minus their Preindustrial control runs (7a-GM\_UNCOR; 7b-GM\_CORR). The patterns are largely similar except in the North and tropical Atlantic where the ocean mixing correction substantially altered SSTs. An intensified hydrological cycle is evident from global increases in both rainfall and evaporation (7c-shown for GM\_CORR only). Note that the colourbar is flipped for the evaporation map so that green shades on all maps indicate a tendency toward wetter conditions while brown indicates drier conditions. Most regional changes in precipitation over land are balanced by evaporation, at least in sign if not in magnitude. In contrast, there are significant regions of the ocean, especially in the subtropics, where the hydrological anomaly in both precipitation and evaporation amplifies the other. The impact on ocean surface salinity needs to be explored with further experiments and analyses.

is calculated by the GCM. Snow depth, while decreasing in the Northern Hemisphere, actually increases on average in the Southern Hemisphere in the Pliocene simulations. This less obvious result is due to the great reduction in circum-Antarctic sea ice, which leads to increased evaporation across warm waters and large increases in snow accumulation over the margins of East Antarctica. Although the West Antarctica Ice Sheet has been removed, and West Antarctica itself is mostly submerged, sea ice formation across that high latitude ocean still forms a platform that allows snow accumulation for much of the year. This begs the question as to whether or not the GISS ModelE2-R would actually support the re-initiation or maintenance of continental glaciation on any portion of West Antarctica.

As mentioned above, the other factor in planetary albedo change is the role of cloud cover. Total cloud cover decreases in the Pliocene, but this is not necessarily an indication of the sign of the feedback, since the vertical distribution of clouds can alter their impact on albedo. However, the vertical profile of cloud changes shown in Fig. 8 strongly suggests that clouds enhance the Pliocene warming, since they decrease on average at every level in the lower and middle troposphere, while increasing slightly near the tropopause. Moist convective cloud cover is the only cloud type to increase in the Pliocene simulations, consistent with the strengthened hydrologic cycle.

Beyond the albedo changes, the atmospheric water vapour increases by about 15 %, providing the typical amplification of the greenhouse effect and another positive feedback that maintains a warmer Pliocene climate. The increased surface area covered by water in the Pliocene plays a role in this increased atmospheric water vapour, but the negative moisture balance across the subtropical ocean expanses of the Southern Hemisphere is a key factor as well (Fig. 7). Intensification of the hydrological cycle results from increases in both rainfall and evaporation rates (+6 %), but annual average precipitation changes over most continental regions are balanced by similarly altered regional patterns of evaporation (at least in sign if not entirely in magnitude). In contrast, there are significant geographic expanses of the subtropics where both precipitation and evaporation change amplifies the effect of the other. The impact on ocean surface salinity may be important to the long-term equilibrium state of Pliocene ocean circulation; we are in the process of conducting longer integrations (beyond these 1000 yr simulations) to explore the issue.

## 6 Conclusions

Given its intriguing potential as a near-analogue to future climate, the mid-Pliocene Warm Period has often been explored by paleoclimatologists and modellers. The interval between 3.3–3.0 million yr ago may truly be the most recent global warming that is anywhere close in magnitude to

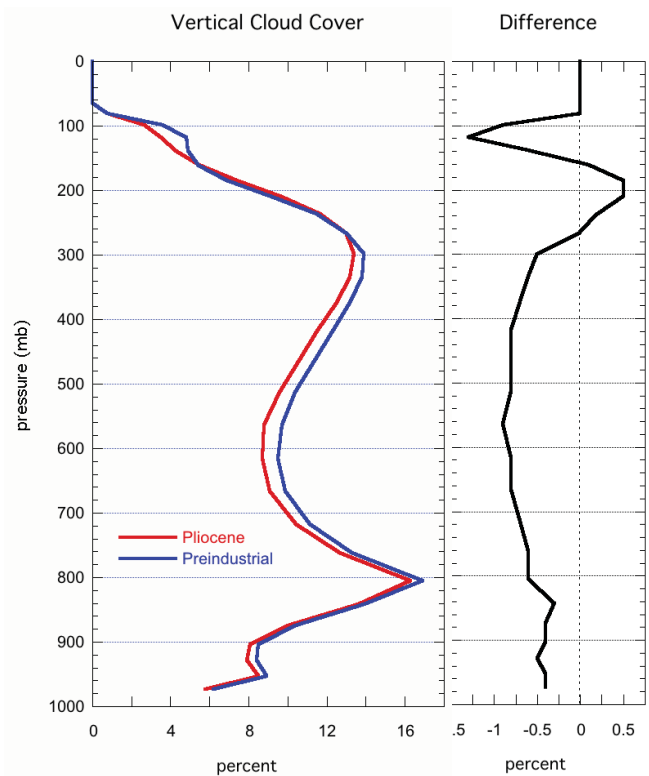


**Fig. 8.** The zonally averaged vertical profile of total cloud cover from the corrected (GM\_CORR) Pliocene and Preindustrial simulations (left plot) and the difference between the two (right plot). Note the separate scales on the x-axes. Changes in cloud cover at all heights are small, but they are consistent. Total cloud cover decreases throughout most of the troposphere and acts as a positive feedback to warming in the Pliocene simulation.

what the Earth faces in its near future. Unfortunately, experiments with many of the coupled ocean-atmosphere models that IPCC relies on for future climate projections have not been fully successful at reproducing the middle Pliocene distribution of warm sea surface temperatures, particularly the strong warming in the far North Atlantic Ocean (Haywood et al., 2013; Dowsett et al., 2012). Numerous proxy studies imply that higher  $\text{CO}_2$  levels are not the sole answer to Pliocene warming, as prior assertions of stable tropical SSTs have been corroborated with each new low-latitude ocean core and each new proxy method.

In this paper, we show preliminary results of the most recent simulations of the mid-Pliocene Warm Period using the latest version (AR5/CMIP5) of the GISS Earth System Model, called ModelE2-R. We discuss two versions of the Pliocene and Preindustrial simulations because one set of simulations includes a post-CMIP5 correction to the model's Gent-McWilliams ocean mixing scheme that has a substantial impact on the results – and offers a substantial improvement, correcting some serious problems with the GISS ModelE2-R ocean. Both Pliocene simulations represent the

NASA/GISS contribution to the Pliocene Model Intercomparison Project (PlioMIP, Experiment 2) and are used in Phase 1 of the PlioMIP multi-model ensemble studies. Going forward, we will adopt only the model version that incorporates the corrected mixing scheme (GM\_CORR in this paper). Many of our results from the Pliocene GM\_CORR simulation fall squarely within the range defined by other coupled models in the PlioMIP ensemble, but we emphasise here some features that would be outliers in the ensemble ranges. The most prominent is the simulation of a large region of warming in the North Atlantic and Greenland-Iceland-Norwegian Sea (large areas covered by SST anomalies greater than  $+4^{\circ}\text{C}$ , with distinct peaks of more than  $9^{\circ}\text{C}$ ). This is by far the most accurate portrayal of this key geographic region by any version of the NASA/GISS family of models to date and comparisons with the Pliocene GM\_UNCOR simulations shows that the ocean mixing scheme correction is the key factor in the improved results – at least for ModelE2-R. There are still model-data differences to be addressed, and these preliminary results require further analysis in order to fully understand the physical processes involved in the warming of the North Atlantic and in the changes to ocean circulation. However, we believe that continued development of key physical routines in the GISS atmospheric model, along with higher resolution and recent corrections made to the Gent-McWilliams mixing parameterisation in the Russell ocean model, have led to an Earth System Model that will produce more accurate projections of both past and future climate.

*Acknowledgements.* The authors acknowledge the support of the NASA High-End Computing (NEC) Program through the NASA Center for Climate Simulation (NCCS) at Goddard Space Flight Center; MAC acknowledges the National Science Foundation Paleoclimate Program Grant No. ATM-0214400; HJD acknowledges the support of the US Geological Survey Climate and Land Use Change R&D Program; HJD and MAC thank the U.S.G.S. Powell Center for Analysis and Synthesis for supporting the PlioMIP initiative.

Edited by: J. C. Hargreaves

## References

- Bender, F. A. M.: Planetary albedo in a strongly forced climate, as simulated by the CMIP3 models, *Theor. Appl. Climatol.*, 105, 529–535, doi:10.1007/s00704-011-0411-2, 2011.
- Chandler, M. A. and Rind, D.: The Influence of Warm North Atlantic Sea Surface Temperatures on the Pliocene Climate: GCM Sensitivity Experiments, EOS, Transactions, American Geophysical Union, 73(14) Supp., 169, 1992.
- Chandler, M. A., Rind, D., and Thompson, R. S.: Joint investigations of the middle Pliocene climate II: GISS GCM Northern Hemisphere results, *Global Planet. Change*, 9, 197–219, doi:10.1016/0921-8181(94)90016-7, 1994.
- Conkright, M. E., Levitus, S., O'Brien, T., Boyer, T. P., Stephens, C., Johnson, D., Stathoplos, L., Baranova, O., Antonov, J., Gelfeld, R., Burney, J., Rochester, J., and Forgy, C.: World Ocean Database 1998 Documentation and Quality Control, National Oceanographic Data Center, Silver Spring, MD, 1998.
- Del Genio, A. D., Yao, M.-S., Kovari, W., and Lo, K. K.-W.: A prognostic cloud water parameterisation for global climate models, *J. Climate*, 9, 270–304, doi:10.1175/1520-0442(1996)009<0270:APCWPF>2.0.CO;2, 1996.
- Dowsett, H. J., Barron, J., and Poore, R.: Middle Pliocene sea surface temperatures: A global reconstruction, *Marine Micropaleontol.*, 27, 13–25, 1996.
- Dowsett, H. J., Robinson, M. M., and Foley, K. M.: Pliocene three-dimensional global ocean temperature reconstruction, *Clim. Past*, 5, 769–783, doi:10.5194/cp-5-769-2009, 2009.
- Dowsett, H., Robinson, M., Haywood, A., Salzmann, U., Hill, D., Sohl, L., Chandler, M., Williams, M., Foley, K., and Stoll, D.: The PRISM3D paleoenvironmental reconstruction, *Stratigraphy*, 7, 123–139, 2010a.
- Dowsett, H. J., Robinson, M. M., Stoll, D. K., and Foley, K. M.: Mid-Piacenzian mean annual sea surface temperature analysis for data-model comparisons, *Stratigraphy*, 7, 189–198, 2010b.
- Galfetti, T., Bucher, H., Brayard, A., Hochuli, P. A., Weissert, H., Guodun, K., Atudorei, V., and Guex, J.: Late Early Triassic climate change: Insights from carbonate carbon isotopes, sedimentary evolution and ammonoid palaeobiogeography, *Palaeogeogr. Palaeoclimatol.*, 243, 394–411, 2007.
- Gent, P. R. and McWilliams, J. C.: Isopycnal mixing in ocean circulation models, *J. Phys. Oceanogr.*, 20, 150–155, 1990.
- Gent, P. R., Willebrand, J., McDougall, T. J., and McWilliams, J. C.: Parameterizing eddy-induced tracer transports in ocean circulation models, *J. Phys. Oceanogr.*, 25, 463–474, 1995.
- Hansen, J. E. and Sato, Mki.: Paleoclimate implications for human-made climate change, in *Climate Change: Inferences from Paleoclimate and Regional Aspects*, edited by: Berger, A., Mesinger, F., and Šijački, D., Springer, Vienna, Austria, 21–48, doi:10.1007/978-3-7091-0973-1\_2, 2012.
- Hansen, J. E., Ruedy, R., Lacis, A., Sato, Mki., Nazarenko, L., Tausnev, N., Tegen, I., and Koch, D.: Climate modelling in the global warming debate. In *General Circulation Model Development*, edited by: Randall, D., Academic Press, 127–164, 2000.
- Hansen, J. E., Sato, Mki., Nazarenko, L., Ruedy, R., Lacis, A., Koch, D., Tegen, I., Hall, T., Shindell, D., Santer, B., Stone, P., Novakov, T., Thomason, L., Wang, R., Wang, Y., Jacob, D., Hollandsworth, S., Bishop, L., Logan, J., Thompson, A., Stolarski, R., Lean, J., Willson, R., Levitus, S., Antonov, J., Rayner, N., Parker, D., and Christy, J.: Climate forcings in Goddard Institute for Space Studies SI2000 simulations, *J. Geophys. Res.*, 107, 4347, doi:10.1029/2001JD001143, 2002.
- Haywood, A. M., Valdes, P. J., and Sellwood, B. W.: Global scale paleoclimate reconstruction of the middle Pliocene climate using the UKMO GCM: initial results, *Global Planet. Change.*, 25, 239–256, 2000.
- Haywood, A. M., Chandler, M. A., Valdes, P. J., Salzmann, U., Lunt, D. J., and Dowsett, H. J.: Comparison of mid-Pliocene climate predictions produced by the HadAM3 and GCMAM3 General Circulation Models, *Global Planet. Change.*, 66, 208–224, 2009.
- Haywood, A. M., Dowsett, H. J., Otto-Bliesner, B., Chandler, M. A., Dolan, A. M., Hill, D. J., Lunt, D. J., Robinson, M. M., Rosen-

- bloom, N., Salzmann, U., and Sohl, L. E.: Pliocene Model Intercomparison Project (PlioMIP): experimental design and boundary conditions (Experiment 1), *Geosci. Model Dev.*, 3, 227–242, doi:10.5194/gmd-3-227-2010, 2010.
- Haywood, A. M., Dowsett, H. J., Robinson, M. M., Stoll, D. K., Dolan, A. M., Lunt, D. J., Otto-Bliesner, B., and Chandler, M. A.: Pliocene Model Intercomparison Project (PlioMIP): experimental design and boundary conditions (Experiment 2), *Geosci. Model Dev.*, 4, 571–577, doi:10.5194/gmd-4-571-2011, 2011.
- Haywood, A. M., Hill, D. J., Dolan, A. M., Otto-Bliesner, B. L., Bragg, F., Chan, W.-L., Chandler, M. A., Contoux, C., Dowsett, H. J., Jost, A., Kamae, Y., Lohmann, G., Lunt, D. J., Abe-Ouchi, A., Pickering, S. J., Ramstein, G., Rosenbloom, N. A., Salzmann, U., Sohl, L., Stepanek, C., Ueda, H., Yan, Q., and Zhang, Z.: Large-scale features of Pliocene climate: results from the Pliocene Model Intercomparison Project, *Clim. Past*, 9, 191–209, doi:10.5194/cp-9-191-2013, 2013.
- Hill, D. J., Haywood, A. M., Hindmarsh, R. C. M., and Valdes, P. J.: Characterising ice sheets during the Pliocene: evidence from data and models, in: *Deep-time perspectives on climate change: marrying the signal from computer models and biological proxies*, edited by: Williams, M., Haywood, A. M., Gregory, J., and Schmidt, D., *Micropalaeontol. Soc., Spec. Pub. Geol. Soc.*, London, 517–538, 2007.
- IPCC: *Climate Change 2007: The Physical Science Basis. Contribution of Working Group I to the Fourth Assessment Report of the Intergovernmental Panel on Climate Change*, edited by: Solomon, S., Qin, D., Manning, M., Chen, Z., Marquis, M., Averyt, K. B., Tignor, M., and Miller, H. L., Cambridge Univ. Press, Cambridge, UK, and New York, 996 pp., 2007.
- Jiang, D. B., Wang, H. J., Ding, Z. L., Lang, X. M., and Drange, H.: Modeling the middle Pliocene climate with a global atmospheric general circulation model, *J. Geophys. Res.-Atmos.*, 110, D14107, doi:10.1029/2004JD005639, 2005.
- Kürschner, W. M., Van der Burgh, J., Visscher, H., and Dilcher, D. L.: Oak leaves as biosensors of late Neogene and early Pleistocene paleoatmospheric CO<sub>2</sub> concentrations, *Mar. Micropaleontol.*, 27, 299–312, 1996.
- Liu, Y. H., Key, J. R., and Wang, X. J.: Influence of changes in sea ice concentration and cloud cover on recent Arctic surface temperature trends, *Geophys. Res. Lett.*, 36, L20710, doi:10.1029/2009GL040708, 2009.
- Lythe, M. B., Vaughn, D. G., and the BEDMAP Consortium: *BEDMAP – bed topography of the Antarctic*, Cambridge, UK, British Antarctic Survey, 2000, Digital media available at: <http://nsidc.org/data/atlas/>, last access: 23 January 2011.
- Matthews, E.: Global vegetation and land use: New high-resolution data bases for climate studies, *J. Clim. Appl. Meteorol.*, 22, 474–487, doi:10.1175/1520-0450(1983)022<0474:GVALUN>2.0.CO;2, 1983.
- Matthews, E.: *Prescription of Land-Surface Boundary Conditions in GISS GCM II: A Simple Method Based on High-Resolution Vegetation Data Bases*, NASA TM-86096, National Aeronautics and Space Administration, 1984.
- Meehl, G. A., Stocker, T. F., Collins, W. D., Friedlingstein, P., Gaye, A. T., Gregory, J. M., Kitoh, A., Knutti, R., Murphy, J. M., Noda, A., Raper, S. C. B., Watters, I. G., Weaver, A. J., and Zhao, Z.-C.: Global Climate Projections, in: *Climate Change 2007: The Physical Science Basis, Contribution of Working Group I to the Fourth Assessment Report of the Intergovernmental Panel on Climate Change*, edited by: Solomon, S., Qin, D., Manning, M., Chen, Z., Marquis, M., Averyt, K. B., Tignor, M., and Miller, H. L., Cambridge University Press, Cambridge, United Kingdom and New York, NY, USA, 2007.
- Pagani, M., Liu, Z. H., LaRiviere, J., and Ravelo, A. C.: High Earth-system climate sensitivity determined from Pliocene carbon dioxide concentrations, *Nat. Geosci.*, 3, 27–30, doi:10.1038/NGEO724, 2010.
- Pearson, P. N., van Dongen, B. E., Nicholas, C. J., Pancost, R. D., Schouten, S., Singano, J. M., and Wade, B. S.: Stable warm tropical climate through the Eocene Epoch, *Geology*, 35, 211–214, 2007.
- Pollard, D. and DeConto, R. M.: Modelling West Antarctic ice sheet growth and collapse through the past five million years, *Nature*, 458, 329–332, 2009.
- Poore, R. Z. and Chandler, M. A.: Simulating past climates, *The data-model connection*, *Global Planet. Change*, 9, 165–167, 1994.
- Raymo, M. E., Grant, B., Horowitz, M., and Rau, G. H.: Mid-Pliocene warmth: Stronger greenhouse and stronger conveyor, *Mar. Micropaleontol.*, 27, 313–326, doi:10.1016/0377-8398(95)00048-8, 1996.
- Redi, M. H.: Oceanic isopycnal mixing by coordinate rotation, *J. Phys. Oceanogr.*, 12, 1154–1158, 1982.
- Rind, D. and Chandler, M. A.: Increased ocean heat transports and warmer climate, *J. Geophys. Res.*, 96, 7437–7461, doi:10.1029/91JD00009, 1991.
- Russell, G. L., Miller, J. R., and Rind, D.: A coupled atmosphere-ocean model for transient climate change studies, *Atmos.-Ocean*, 33, 683–730, 1995.
- Salzmann, U., Haywood, A. M., Lunt D. J., Valdes, P. J., and Hill, D. J.: A new Global Biome Reconstruction and Data-Model Comparison for the middle Pliocene, *Global Ecol. Biogeogr.*, 17, 432–447, 2008.
- Schmidt, G. A., Ruedy, R., Hansen, J. E., Aleinov, I., Bell, N., Bauer, M., Bauer, S., Cairns, B., Canuto, V., Cheng, Y., Del Genio, A., Faluvegi, G., Friend, A. D., Hall, T. M., Hu, Y., Kelley, M., Kiang, N. Y., Koch, D., Lacis, A. A., Lerner, J., Lo, K. K., Miller, R. L., Nazarenko, L., Oinas, V., Perlwitz, J. P., Perlwitz, Ju., Rind, D., Romanou, A., Russell, G. L., Sato, M., Shindell, D. T., Stone, P. H., Sun, S., Tausnev, N., Thresher, D., and Yao, M.-S.: Present day atmospheric simulations using GISS ModelE: Comparison to in-situ, satellite and reanalysis data, *J. Climate*, 19, 153–192, doi:10.1175/JCLI3612.1, 2006.
- Schmidt, G. A., Kelley, M., Nazarenko, L., Ruedy, R., Russell, G. L., Aleinov, I., Bauer, M., Bauer, S., Bhat, M. K., Bleck, R., Canuto, V., Chen, Y., Ye Cheng, Clune, T. L., Del Genio, A., de Fainchtein, R., Faluvegi, G., Hansen, J. E., Healy, R. J., Kiang, N. Y., Koch, D., Lacis, A. A., LeGrande, A. N., Lerner, J., Lo, K. K., Marshall, J., Menon, S., Miller, R. L., Oinas, V., Olos, A. O., Perlwitz, J., Puma, M. J., Putman, W. M., Rind, D., Romanou, A., Sato, M., Shindell, D. T., Shan Sun, Syed, R. A., Tausnev, N., Tsigaridis, K., Unger, N., Voulgarakis, A., Mao-Sung Yao, and Jinlun Zhang: Configuration and assessment of the GISS ModelE2 contributions to the CMIP5 archive, in preparation, 2013.
- Scroton, N., Bonham, S. G., Rickaby, R. E. M., Lawrence, S. H. F., Hermoso, M., and Haywood, A. M.: Persistent El Niño–Southern Oscillation variation during the Pliocene Epoch, *Paleoceanogra-*

- phy, 26, PA2215, doi:10.1029/2010PA002097, 2011.
- Seki, O., Foster, G. L., Schmidt, D. N., Mackensen, A., Kawamura, K., and Pancost, R. D.: Alkenone and boron-based Pliocene pCO<sub>2</sub> records, *Earth Planet. Sci. Lett.*, 292, 201–211, 2010.
- Shukla, S. P., Chandler, M. A., Jonas, J., Sohl, L. E., Mankoff, K., and Dowsett, H.: Impact of a permanent El Niño (El Padre) and Indian Ocean Dipole in warm Pliocene climates, *Paleoceanography*, 24, PA2221, doi:10.1029/2008PA001682, 2009.
- Shukla, S. P., Chandler, M. A., Rind, D., Sohl, L. E., Jonas, J., and Lerner, J.: Teleconnections in a warmer climate: The Pliocene perspective, *Clim. Dynam.*, 37, 1869–1887, doi:10.1007/s00382-010-0976-y, 2011.
- Sloan, L. C., Crowley, T. C., and Pollard, D.: Modeling of middle Pliocene climate with the NCAR GENESIS general circulation model, *Mar. Micropaleontol.*, 27, 51–61, 1996.
- Sohl, L. E., Chandler, M. A., Schmunk, R. B., Mankoff, K., Jonas, J. A., Foley, K. M., and Dowsett, H. J.: PRISM3/GISS topographic reconstruction, *U. S. Geol. Surv. Data Series*, 419, 6 pp., 2009.
- Tang, Q. H., Leng, G. Y., and Groisman, P. Y.: European hot summers associated with a reduction of cloudiness, *J. Climate*, 25, 3637–3644, doi:10.1175/JCLI-D-12-00040.1, 2012.
- Visbeck, M., Marshall, J., Haine, T., and Spall, M.: Specification of Eddy Transfer Coefficients in Coarse-Resolution Ocean Circulation Models, *J. Phys. Oceanogr.*, 27, 381–402, doi:10.1175/1520-0485(1997)027<0381:SOETCI>2.0.CO;2, 1997.
- Wang, H. L. and Lau, K. M.: Atmospheric hydrological cycle in the tropics in twentieth century coupled climate simulations, *Int. J. Climatol.*, 26, 655–678, 2006.
- Watanabe, T., Suzuki, A., Minobe, S., Kawashima, T., Kameo, K., Minoshima, K., Aguilar, Y. M., Wani, R., Kawahata, H., Sowa, K., Nagai, T., and Kase, T.: Permanent El Niño during Pliocene warm period not supported by coral evidence, *Nature*, 471, 209–211, doi:10.1038/nature09777, 2011.
- Zachos, J. M., Scott, L. D., and Lohmann, K. C.: Evolution of early Cenozoic marine temperatures, *Paleoceanography*, 9, 353–387, 1994.
- Zhang, Z.-S., Nisancioglu, K. H., Chandler, M. A., Haywood, A. M., Otto-Bliesner, B. L., Ramstein, G., Stepanek, C., Abe-Ouchi, A., Chan, W.-L., Bragg, F. J., Contoux, C., Dolan, A. M., Hill, D. J., Jost, A., Kamae, Y., Lohmann, G., Lunt, D. J., Rosenbloom, N. A., Sohl, L. E., and Ueda, H.: Mid-pliocene Atlantic meridional overturning circulation not unlike modern?, *Clim. Past Discuss.*, 9, 1297–1319, doi:10.5194/cpd-9-1297-2013, 2013.